ASMS

RESEARCH ARTICLE

Sulfur Transfer Versus Phenyl Ring Transfer in the Gas Phase: Sequential Loss of CH$_3$OH and CH$_3$O–P=O from Protonated Phosphorothioates

Xiaoping Zhang,[1] Honghan Chen,[1] Yin Ji,[1] Kezhi Jiang,[2] Huanwen Chen[1]

[1]Jiangxi Key Laboratory for Mass Spectrometry and Instrumentation, East China University of Technology, Nanchang, 330013, People's Republic of China
[2]Key Laboratory of Organosilicon Chemistry and Material Technology, Hangzhou Normal University, Hangzhou, 311121, China

sulfur transfer *vs* phenyl transfer
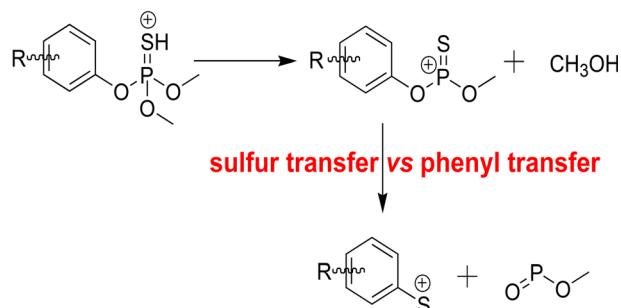
Abstract. Collisional activation fragmentation of protonated phosphorothioates leads to skeletal rearrangement and formation of aryl sulfenylium cation (R-PhS$^+$) via successive eliminations of CH$_3$OH and CH$_3$O–P=O. To better understand this unusual fragmentation reaction, isotope-labeling experiments and density functional theory (DFT) calculations were carried out to investigate two mechanistic pathways. In route 1, a direct intramolecular transfer of the R-phenyl group occurs from the oxygen atom to the sulfur atom on thiophosphoryl to form methoxyl *S*-(3-methyl-4-methylsulfanyl-phenyl) phosphonium thiolate (**a4**), which subsequently dissociates to form the *m/z* 169 cation. In route 2, the sulfur atom of the thiophosphoryl group undergoes two stepwise transfer (1,4-migration to the *ortho*-carbon atom of the phenyl ring followed by 1,2-migration to the *ipso*-carbon atom) to form an intermediate isomer, which undergoes the subsequent dissociation to form the *m/z* 169 cation. DFT calculations suggested that route 2 was more favorable than route 1 from the point view of kinetics.

Keywords: Sulfur transfer, Phenyl ring transfer, Tandem mass spectrometry, Phosphorothioates, Benzenesulfenylium cation

Introduction

The combination of electrospray ionization mass spectrometry (ESI-MS) with collision-induced dissociation (CID) is commonly used to study the properties of gas-phase ions and mechanisms of gas-phase reactions [1–6]. However, the interpretation of CID spectra is not always straightforward due to various rearrangements that occur during fragmentation [7–14]. The reported rearrangements in the gas-phase included benzyl cation transfer, sulfonyl cation transfer, and halogen

transfer, and have been a subject of many mechanistic studies [7–22].

Sulfur transfer reactions have been increasingly used in organic synthesis [23–27]. Among this class of rearrangement reactions, 1,2-sulfur transfer has been widely investigated and extensively used in the synthesis of heterocycles [23, 28, 29] and in carbohydrate chemistry [30, 31]. The most common pathway of 1,2-sulfur transfer proceeds through a key thiiranium intermediate, which can either undergo elimination to give allyl thioethers or substitution to generate formally transposed substitution products [25]. Other types of sulfur transfer, such as 1,3-sulfur transfer [24] and 1,4-sulfur transfer [32], are rarely described. To the best our knowledge, however, no report has been found on the gas-phase intramolecular sulfur transfer reaction, which deserves further investigation.

Phosphorothioates bearing an S=P bond display important chemical and biological properties that afford utility in various

Correspondence to: Kezhi Jiang; *e-mail:* jiankezhi@hznu.edu.cn, Huanwen Chen; *e-mail:* chw8868@gmail.com

fields, including organic synthesis, medicinal chemistry, molecular biology, and agrochemistry [33, 34]. Previous studies mainly focused on the determination and quantification of phosphorothioates, while few studies focused on their gasphase fragmentation [35–39]. As an example, a thiono-thiolo rearrangement (Newman-Kwart rearrangement), where the S=P–OR group rearranges to the O=P–SR group via R- transfer, can occur under electron ionization or tandem MS [36, 37]. A curious R-PhS$^+$ type of ion was observed in the fragmentation of protonated fenthion [36, 40, 41], but no detailed mechanism has been documented to our knowledge. In this work, an intriguing rearrangement reaction to the formation of R-PhS$^+$ ion via sulfur transfer has been investigated in the ESI-MS analysis of phosphorothioates. The mechanism of this reaction was examined in detail by a combination of experimental and theoretical calculation approaches.

Experimental Section

Chemicals and Material

Methanol HPLC grade was purchased from Sigma-Aldrich (St. Louis, MO, USA). Fenthion, parathion-methyl (compound 2), fenitrothion (compound 3), tolclofos-methyl (compound 4), and chlorpyrifos-methyl (compound 5) were purchased from J&K Scientific Ltd. (Shanghai, China) with a purity >99%.

Mass Spectrometry

The samples were analyzed on an LTQ-XL advantage IT-MS (Theromo Scientific, San Jose, CA, USA) and an Orbitrap-XL mass spectrometer (Theromo Scientific, San Jose, CA, USA) using a home-made ESI interface in the positive ion mode. Every diluted solution (1 µg mL^{-1} in methanol) was infused into the source chamber at a flow rate of 3 µL min^{-1}. The optimized ESI source conditions were as follows: the ion-spray voltage, 3 kV; the nebulizing gas (N$_2$), 25 arbitrary units (a.u.); the capillary temperature, 150 °C, the capillary voltage in 80 V; the tube lens in 100 V. Other parameters were automatically optimized by the system. The ion trap pressure of approximately 1 × 10^{-5} Torr was maintained with a Turbo pump and pure helium (99.99%) was used as the collision gas. The instrument was operated at a high resolution up to 100,000. The CID-MS experiments were performed by using an excitation AC voltage to the end caps of the ion trap to include collisions of the isolated ions (isolation width at 1 m/z) for a period of 30 ms and variable excitation amplitudes. The CID-MS spectra of the protonated molecules were obtained by activation of the precursor ions at the normalized collision energy of 15%~30%.

Theoretical Calculations

Theoretical calculations were performed using the Gaussian 09 program [42]. The geometries of reactants, transition states, intermediates, and products were optimized using the density functional theory (DFT) method at the B3LYP/6-31+G(d,p) level. All reactants, intermediates, and products were identified as true minima in energy by the absence of imaginary frequencies. Transition state (TS) structures were obtained through relaxed PES scans utilizing DFT method at the B3LYP/6-31+G(d,p) level to generate initial structures for the TSs, in which a bond length was scanned to find a first-order saddle point, and subsequently optimizing the corresponding transition state. Then, the relevant TS structures are searched and optimized using either TS or QST2 procedures. QST2 uses a quadratic synchronous transit approach to get closer to the quadratic region of the TS and then uses a quasi-Newton algorithm to complete the optimization. All transition states were confirmed by the presence of a single imaginary vibrational frequency and the reasonable vibrational mode. Intrinsic reaction coordinate (IRC) calculations at the same level of theory were performed on each transition state to further confirm that the optimized TS structures were actually connected to the correct reactants and products by a steepest descend path. Vibrational frequencies of all the key species were calculated at the same level of theory. Full structural details and energies of all structures involved are available in the supplementary material. The energies discussed here are the sum of electronic and thermal free energy.

Result and Discussion

Fragmentation Behavior of Protonated Fenthion

The gas phase sulfur transfer rearrangement reaction was explored by investigating the MS fragmentation behavior of protonated fenthion derivatives. Fenthion (compound 1) was selected as a model to perform a detailed investigation. The tandem mass spectrum of protonated fenthion (the mass-isolated m/z 279) shown in Figure 1 reveals the formation of a dominant fragment ion at m/z 247, corresponding to methoxyl O-(3-methyl-4-methylsulfanyl-phenyl) phosphonium thioate, a3 (Supplementary Material Scheme S1) via a neutral loss of 32 Da (methanol). Three minor fragment ions are observed at m/z 231 (b2), m/z 169 (a8), and m/z 137 (b1), corresponding to the neutral losses of 48 Da, 110 Da, and 142 Da, respectively (Figure 1(a)). The neutral loss of 48 Da likely arises from elimination of methanethiol. The fragment ion at m/z 137 is assigned as 3-methyl-4-methylsulfanyl-benzene cation (Scheme S1), which can be attributed to the loss of O,O'-dimethyl thiophosphate from the precursor ion at m/z 279. The fragment ion at m/z 169 is attributed to 3-methyl-4-methylsulfanyl-benzenesulfenylium cation (Scheme S1) or its isomer, resulted from the elimination of C$_2$H$_7$O$_3$P of the precursor ion, which will be discussed in detailed in the following sections. The elemental compositions of these products were confirmed by accurate mass measurements performed on a high-resolution Orbitrap-XL mass spectrometer (Supplementary Material Figure S1 and Table S1).
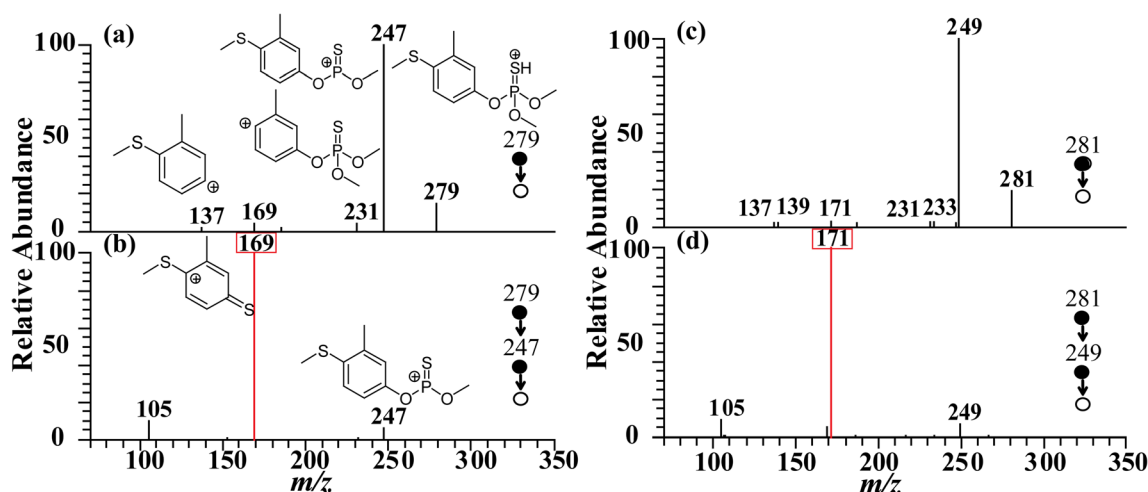
Figure 1. Collision-induced dissociation mass spectra of [1 + H]$^+$ at the normalized collision energy of 16%. (a) MS^2 spectrum of [1 + H]$^+$ (m/z 279 →), (b) MS^3 spectrum of [1 + H]$^+$ (m/z 279 → m/z 247 →), (c) MS^2 spectrum of [1-^{34}S + H]$^+$ (m/z 281 →), (d) MS^3 spectrum of [1-^{34}S + H]$^+$ (m/z 281 → m/z 249 →)

Fragmentation Pathways to R-benzenesulfenylium Cation

The characteristic fragment ion at m/z 169 can only be interpreted as a result of the $C_2H_7O_3P$ elimination via sulfur transfer. To interpret the structure of the ion at m/z 169, the MS^3 experiments were performed. As shown in Figure 1(b), the MS^3 spectrum of protonated fenthion (m/z 279 → m/z 247 →) shows a base peak ion at m/z 169 via successive eliminations of CH_3OH (32 Da) and $CH_3OP=O$ (78 Da). However, there is no relevant moiety of $CH_3OP=O$ in the structure of **a3**. Thus, the generation of the ion at m/z 169 originated from dissociation of **a3** (m/z 247) via skeletal rearrangement.
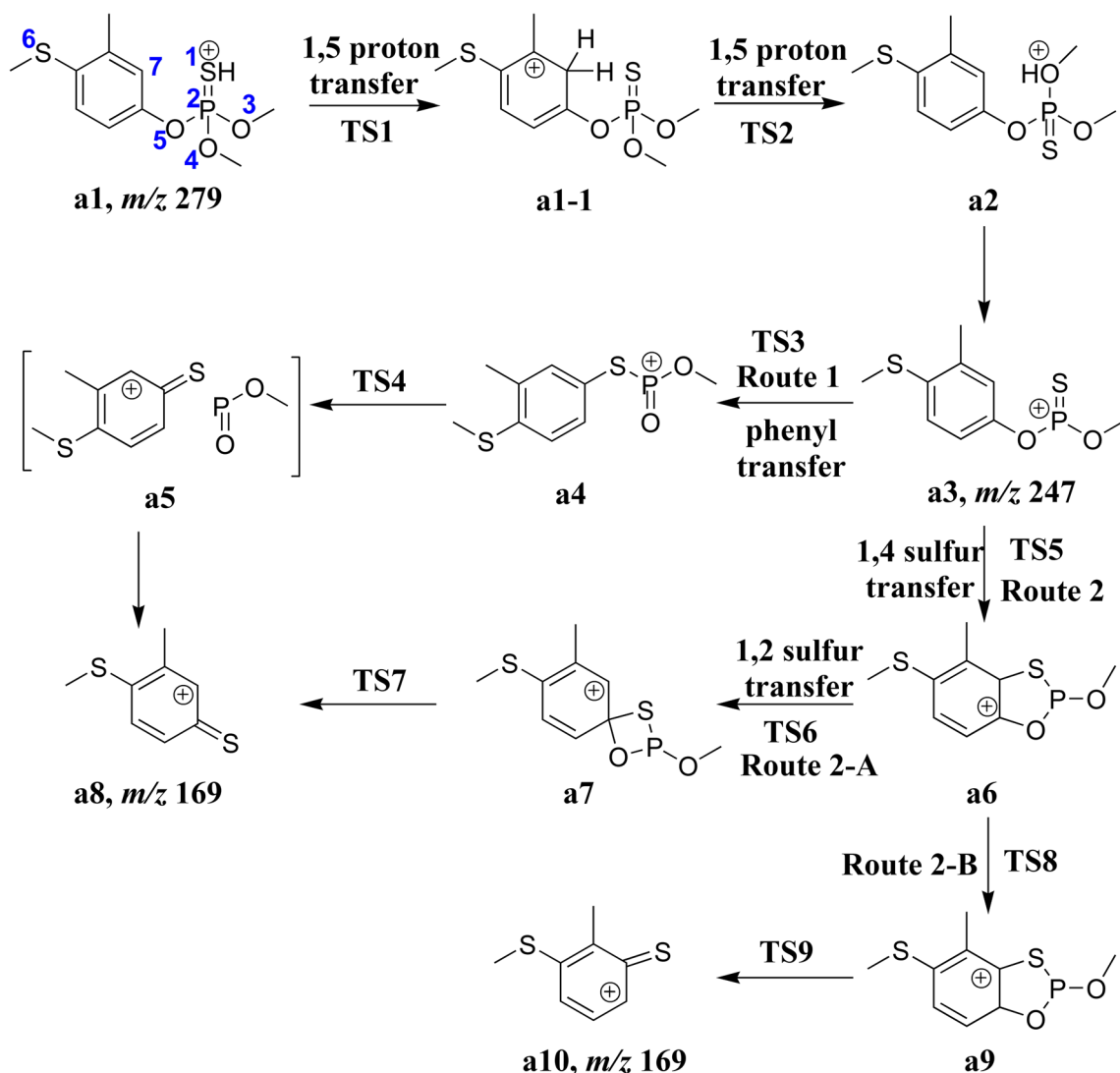
Two potential pathways for the generation of m/z 169 from **a3** were proposed in Scheme 1. In route 1, a direct transfer of 1-methyl-2-methylsulfanyl-benzene group to **S1** atom leads to an intermediate **a4** (methoxyl S-(3-methyl-4-methylsulfanyl-phenyl) phosphonium thiolate), which undergoes the subsequent dissociation to form **a8** at m/z 169. An analogous intramolecular O- to S-benzene migration has also been reported in the gas phase fragmentation diphenyl phosphorochloridothioate using electron impact MS by Cooks [37]. In route 2, the *ortho*-carbon atom of the phenyl ring firstly undergoes a nucleophilic attack on the positively charged P=S group, which leads to a bicyclic intermediate **a6**. Then, the **S1** atom in a **a6** undergo a 1,2-migration to form a spiro intermediate **a7**, which subsequently undergoes the dissociation to give **a8** by lose of $CH_3O–P=O$ (route 2-A), or the H atom in **C7** undergo a 1,2-migration to form a bicyclic intermediate **a9**, which subsequently undergoes the dissociation to generate **a10** by elimination of $CH_3O–P=O$ (route 2-B).

The potential pathways in Scheme 1 lead to the product ion at m/z 169 with the structure 3-methyl-4-methylsulfanyl-benzenesulfenylium cation or 2-methyl-3-methylsulfanyl-benzenesulfenylium cation. Benzene-sulfenylium cations have been generated in high abundance by ionization of different precursors containing a thiophenyl group and their gas-phase

reactivity has also been reported [14, 43]. Two approaches have been proposed to prepare sulfonium cations. One is unimolecular sulfur-heteroatom bond fission of "cationoid" complexes or "carriers" of sulfonated compounds, a process usually attempted in the presence of strong Lewis acids [44]. The other approach involves the single-electron oxidation of disulfides [45]. The arylthio group (ArS) is of intrinsic interest and has long been incorporated into drug molecules and peptides, which can exhibit highly activities such as antiplasmodial activity, and antiviral activity [46–48]. Thus, it is of considerable interest to investigate the mechanistic formation of the benzenesulfenylium cation (m/z 169).

Native ^{34}S Isotope and Isotope Labeling Experiments

The postulated decomposition reactions in Scheme 1 were confirmed by the MS/MS analysis on the native ^{34}S isotopic ion (Figure 1(c), (d)) [49]. The sulfur element has two isotopes, ^{32}S and ^{34}S in nature, with the relative abundance at 100% and 4.4%, respectively. As shown in Scheme S1, decomposition of the mono isotope ion of **a1** (MH$^+$) at m/z 279 produces the fragment ion **b2** at m/z 231 by lose of CH_3SH. The first ^{34}S isotope ion at m/z 281, however, contains two isomeric structures (**a1-I1** and **a1-I2** in Scheme S2), due to the different position of ^{34}S. As expected, fragmentation of isomer **a1-I1** gives the product ion **b2-I1** at m/z 233, through the neutral loss of $CH_3{}^{32}SH$; whereas dissociation of isomer **a1-I2** results in the product ion **b2-I2** at m/z 231 *via* the neutral loss of $CH_3{}^{34}SH$. The almost identical abundance of the two product ions is attributed to the equal distribution of the ^{34}S atom in nature. Interestingly, elimination of $S=P(OH)(OCH_3)_2$ from the isotopic ion at m/z 281 shows similar fragmentation behavior, with nearly equivalent abundance of the isotopic fragment ions at m/z 137 and m/z 139. The fragment **b2-I1** (m/z 137) is generated by the dissociation of isomer **a1-I1** through lose of $^{34}S=P(OH)(OCH_3)_2$, while the product ion **b2-I2** (m/z 139) is

Scheme 1. Proposed pathways for the generation of the ions at *m/z* 247 and *m/z* 169

formed *via* S=P(OH)(OCH$_3$)$_2$ elimination from **a1-I2**. The product ion of **a3** *m/z* 247 (or **a8/a10** at *m/z* 169), however, has two sulfur atoms in the chemical formula, and thus both appear as the mono isotopic ion peak with an increasing mass shift of 2 Da in the CID spectrum. Similarly, as shown in Figure 1(d), an increasing mass shift of 2 Da was observed for **a8/a10** (from *m/z* 169 to *m/z* 171) in the MS^3 spectrum of protonated ^{34}S isotopologue (*m/z* 281 → *m/z* 249 →).

The proposed dissociation pathways in Scheme 1 were also supported by the CID-MS analysis of the deuterium-labeling ion (Figure 2). As shown in Scheme 1, there is no external proton in the product ion **a3**, and thereby dissociation of [1 + H]$^+$ and [1 + D]$^+$ theoretically resulted in **a3** with the same mass (247 Da). However, both the ions at *m/z* 248 and *m/z* 247 were observed in the CID mass spectrum of [1 + D]$^+$, corresponding to the loss of CH$_3$OH and CH$_3$OD, respectively. The existence of the ion at *m/z* 248 implies that an H/D exchange in the fragmentation process, e.g. exchange of the external deuteron to the *ortho*-positions of phenyl ring via a six-membered ring. After the deuteron transfers to phenyl ring, the proton or

deuteron may migrate back to the methoxyl oxygen competitively, which results in subsequent losses of CH$_3$OH and CH$_3$OD, respectively. The subsequent transfer of a proton or a deuteron on **a1-1** via **TS2** for the reaction to proceed was marked by a considerable kinetic isotope effect, k_H/k_D. The intensity ratio of elimination of CH$_3$OH (*m/z* 248) to elimination of CH$_3$OD (*m/z* 247) is about 5:1, which represents the majority of their k_H/k_D value. Our results are consistent with reports of kinetic isotope effect in the range of $k_H/k_D = 5$ during the interannular proton transfer steps of benzylbenzenium ions and 1,4-diphenyl-but-2-yne ions [50].

Density Functional Theory Calculations

To further investigate the mechanisms associated with the sulfur and benzene migration reactions, density functional theory (DFT) calculations were carried out at the B3LYP/6-31+G(d,p) level of theory. A lone pair of electrons of a heteroatom is much easier to capture proton [35]. Thus, there are multiple potential protonation sites for fenthion, including *S1*
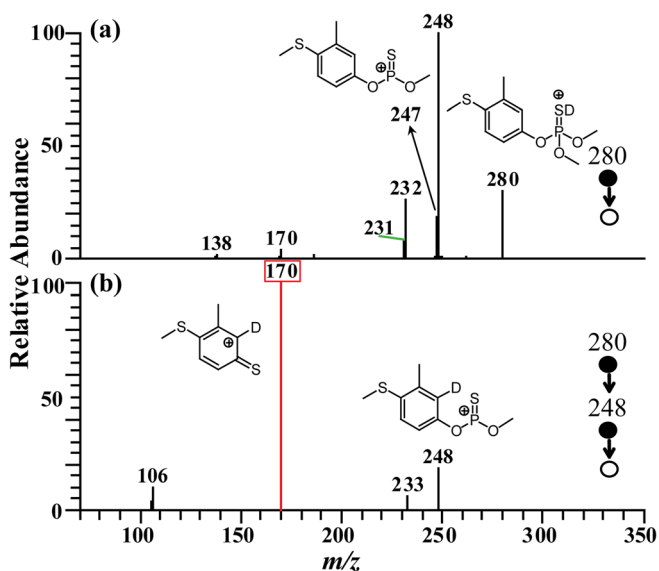
Figure 2. Collision-induced dissociation mass spectra of [1 + D]$^+$. (**a**) MS^2 spectrum of [1 + D]$^+$ (m/z 280 →), (**b**) MS^3 spectrum of [1 + D]$^+$ (m/z 280 → m/z 248 →)
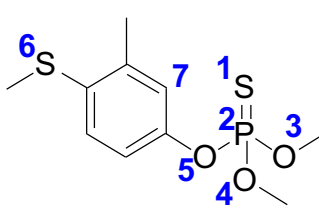
of the thiophosphoryl, **O3/O4** of the methoxy, **O5** of the phenoxy, and **S6** of the methyl sulfide (Table 1). The structures with different protonation sites of fenthion were optimized at the same level (B3LYP/6-31+G(d,p)) and the relative energies of these structures are summarized in Table 1. Overall, the calculation results indicates that **S1** atom is the most thermo-dynamically favorable protonation site, which is 41.3 kJ/mol, 86.4 kJ/mol, 79.7 kJ/mol, and 45.0 kJ/mol lower than proton-ation site on **S6** atom, **O3/O4** atom, **O5** atom, and **C7** atom, respectively. It has been extensively accepted that the ionizing proton can transfer to other less favored sites during the sub-sequent fragmentation process [17, 19].

Figure 3 shows a schematic potential energy surface plot for the generation of **a3** (m/z 247). Firstly, the external proton in **a1** undergoes a 1,5-migration to the *ortho*-carbon atom of the phenyl ring via a six-membered ring transition state (**TS1**) to afford an isomer **a1-1**. This process only needs to surmount an energy barrier of 59.9 kJ mol^{-1}. Then, the activated proton at the *ortho*-carbon atom of the phenyl ring undergoes 1,5-

migration back to the oxygen atom (**O3/O4**) of the methoxy group to afford an isomer **a2** via a six-membered ring transition state (**TS2**), which surmounts an energy barrier of 111.0 kJ mol^{-1}. The oxygen atom of the methoxy group in **a2** is charged trivalent oxygen atom. When **a2** ion is formed, theoretical calculations indicates that breakage of the **P2**–**O3/O4** bond occurs spontaneously, and the two formed fragments are still held together electrostatically as a stable ion-neutral complex (INC) [**a3**/methanol] with a stabilization energy of 49.2 kJ mol^{-1}. A direct decomposition of [**a3**/methanol] results in the formation of **a3**.

The two potential routes to the ion at m/z 169 in the subse-quent fragmentations of **a3** were compared by theoretical cal-culations (Figure 4), and details of the corresponding structures are available in the Supplementary Material. In route 1, the phenyl ring in **a3** is transferred from **O5** to **S1** through a four-membered ring transition state (**TS3**), leading to the formation of **a4** ion with a new carbon-sulfur bond. This process needs to surmount an energy barrier of 168.3 kJ mol^{-1}. The rearrange-ment occurs with a concerted process with cleavage of C–O bond and formation of C–S bond, which can be viewed as an electrophilic substitution of the phenyl ring (Figure 5). The conversion of *O*-aryl carbamothioates to *S*-aryl carbamothioates in the solution-phase is called Newman-Kwart rearrangement, which is an efficient method for the straightforward preparation of thiophenol from the correspond-ing phenols [51]. Migration of phenyl from oxygen to sulfur has also been observed in spectra of sulphonyl derivatives and dimethylthiocarbamates in the gas phase [52]. The free energy of **a4** ion is 8.8 kJ mol^{-1} lower than that of **a3** ion. Then, the formed **a4** continues to undergo the cleavage of the P–S bond induced by the positive charge in **P2** atom, and gives rise to an INC intermediate **a5** [3-methyl-4-methylsulfanyl-benzenesulfenylium cation/metaphosphorous acid methyl es-ter] with a small energy barrier of 15.2 kJ mol^{-1} (**TS4**). The free energy of intermediate **a5** is 20.2 kJ mol^{-1} lower than that of **a3** ion. The sum free energy of the separated ion **a8** and metaphosphorous acid methyl ester is higher than that of **a5** by 46.0 kJ mol^{-1}; this indicates that **a5** seems relatively stable from the view of stabilization energy.

Table 1. Relative energies of [1 + H]$^+$ ions with different protonation sites

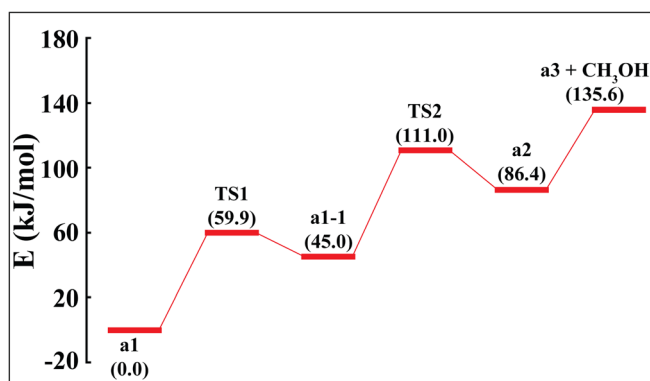| Compound 1	Site of protonation	Relative energy (kJ mol^{-1})
	S1 of the thiophosphoryl	0.0
	O3/O4 of the methoxy	86.4
	O5 of the phenoxy	79.7
	S6 of the methyl sulfide	41.3
	C7 of the phenyl ring	45.0

Figure 3. Potential energy diagram for the generation of *m/z* 247

In route 2, the *ortho*-carbon atom of the phenyl ring firstly undergoes a nucleophilic attack on the positively charged P=S group via a five-membered ring transition state (**TS5** in Figure 5), and affords a bicyclic intermediate **a6**. This process only needs to surmount the energy barrier of 88.1 kJ mol^{-1}. As shown in Figure 5, the length of P–S bond is increased to 2.055 Å in **TS5**, which appreciably longer than a P=S bond (1.887 Å) and shorter than a covalent P–S bond (2.209 Å). The reason for the elongation of P=S bond in **a3** is the formation of five-membered ring by nucleophilic attack of the ring double bond on the positively charged P=S group. The free energy of **a6** ion is 18.0 kJ mol^{-1} lower than that of **a3** ion, indicating a more stable structure.

Interestingly, a subsequent 1,2-sulfur transfer in **a6** occurs through a three-membered ring transition state (**TS6**) to afford **a7**, with a small energy barrier of 59.9 kJ mol^{-1} (in route 2-A). This sulfur scrambling process is similar to proton scrambling on the phenyl ring [20]. The lengths of two C–S bonds involving sulfur scrambling in **TS6** are 2.169 Å and 2.063 Å, respectively. Both are longer than that of a covalent C–S bond (1.738 Å, Figure 5). The four-membered ring structure of **a7** seems less stable than the five-membered ring structure of **a6**. Thus, the ion **a7** subsequently undergoes the loss of metaphosphorous acid methyl ester via simultaneous cleavage of the P–S bond and C–O bond (Figure 5). This step is the key step in route 2-A, which surmounts an energy barrier of
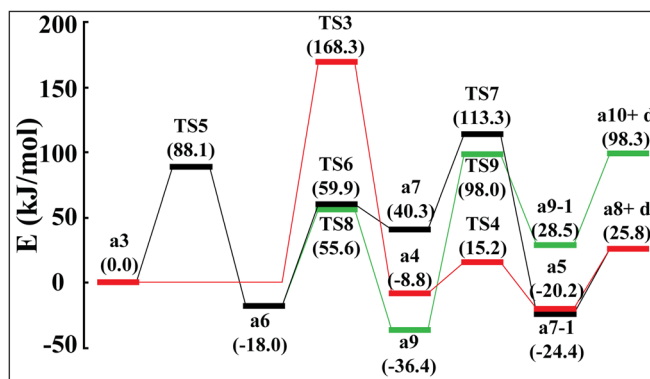
113.3 kJ mol^{-1} (**TS7**). The rearrangement mechanism in route 2-A can be viewed as a successive stepwise of 1,4-sulfur transfer and 1,2-sulfur transfer, then forming a stable 3-methyl-4-methylsulfanyl-benzenesulfenylium cation (**a8**) via open-ring reaction accompanied by the cleavage of the P–S bond and C–O bond.

Alternatively, a subsequent 1,2-proton transfer in **a6** occurs through a three-membered ring transition state (**TS8**) to afford **a9**, with a small energy barrier of 55.6 kJ mol^{-1} (in route 2-B). Then, the ion **a9** subsequently undergoes the elimination of metaphosphorous acid methyl ester via direct cleavage of the P–S bond and C–O bond (**TS9**). This step is the key step in route 2-B, which surmounts an energy barrier of 98.0 kJ mol^{-1} (**TS9**). Thus, the rearrangement mechanism of route 2-B can be viewed as a successive stepwise of 1,4-sulfur transfer and 1,2-proton transfer, then forming a stable 2-methyl-3-methylsulfanyl-benzenesulfenylium cation (**a10**) via open-ring reaction accompanied by the cleavage of the P–S bond and C–O bond.

The key energy barriers of route 2-A (113.3 kJ mol^{-1}) and route 2-B (98.0 kJ mol^{-1}) are much lower than that of route 1 (phenyl migration, 168.3 kJ mol^{-1}), indicating that sulfur migration is a kinetically more favored process than phenyl migration in the formation of ion at **a8** (*m/z* 169). For route 2-A and route 2-B, the minimum activation energy for the cleavage of the P–S bond and C–O bond process via **TS7** and **TS9** is 73.0 kJ mol^{-1} and 134.4 kJ mol^{-1}, respectively, indicating a kinetically more favorable process of route 2-A. Additionally, the sum free energy of the separated ion **a8** and metaphosphorous acid methyl ester is 72.5 kJ mol^{-1} less than that of the separated ion **a10** and metaphosphorous acid methyl ester; this indicates that formation of **a8** is a thermodynamically favored process. Thus, the formation of **a8** in route 2-A is the major path.

The energy requirements for the formation of **a8** and metaphosphorous acid methyl ester are 25.8 kJ mol^{-1} higher than that of **a3**. However, the free energy of **a7-1** is 50.2 kJ mol^{-1} lower than that of the separated ion **a8** and metaphosphorous acid methyl ester; this indicates that **a7-1** seems relatively stable from the view of stabilization energy. In addition, the minimum internal excess energy of **a7-1** is 137.7 kJ mol^{-1} or at least 87.5 kJ mol^{-1} above the separation energy. Thus, direct separation of **a7-1** easily occurs in terms of energy, which generates an abundance of ion at *m/z* 169 (**a8**).

The Universality of the Gas-Phase Sulfur Transfer

To better delineate the universality of this gas-phase sulfur migration reaction, NO$_2$-substituted (compounds **2** and **3**) and Cl-substituted (compounds **4** and **5**) derivatives of fenthion were also investigated by tandem MS experiments, and the tandem MS data (Supplementary Material Figures S2, S3, and S4) were summarized in Table 2. All of these compounds show similar fragmentation behaviors in the MS/MS experiments. Noteworthily, the intensive fragment ions of the corresponding **a8** (*m/z* 154, *m/z* 168, *m/z* 191, and *m/z* 212 for compounds **2**, **3**, **4**, and **5**, respectively) were observed for all compounds.
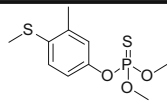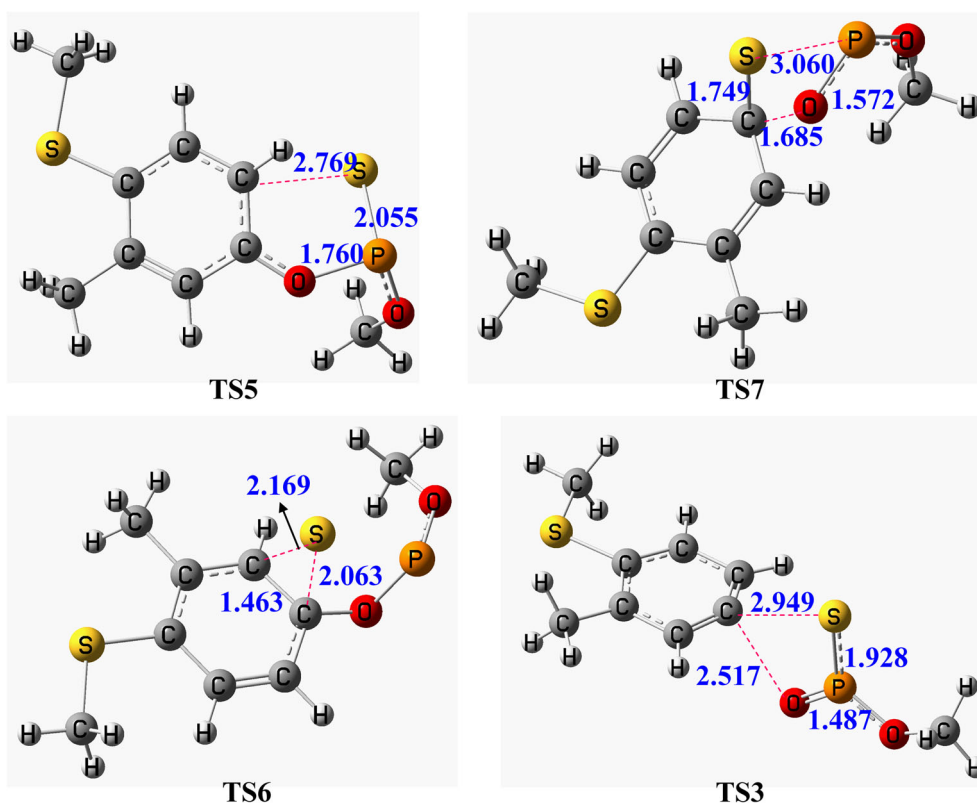

Figure 4. Potential energy diagram for the generation of *m/z* 169. (red line: route 1, black line: route 2-A, green line: route 2-B, d: metaphosphorous acid methyl ester)
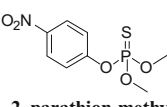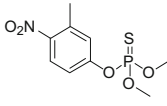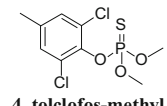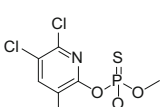
Figure 5. The optimized structures of key intermediates. The bond lengths are given in Å

Table 2. The collision-induced dissociation mass spectra data of $[M + H - CH_3OH]^+$ from protonated fenthion derivatives (**1–5**)

Compounds	$[M + H]^+$ m/z	$[M + H - CH_3OH]^+$ m/z (%)	Loss of 78 Da m/z (%)	Other ions m/z (%)
1, fenthion	279	247(5)	169(100)	105(10)
	281	249(5)	171(100)	105(10)
2, parathion-methyl	264	232(10)	154(3)	202(100), 200(20), 186(28), 172(7)
3, fenitrothion	278	246(2)	168(13)	216(20), 214(10), 200(50), 182(20)
4, tolclofos-methyl	301	269(10)	191(65)	254(60), 237(50), 187(80), 175(100)
	303	271(25)	193(70)	256(60), 239(50), 187(42), 189(43), 177(100)
	305	273(60)	273(85)	258(72), 241(40), 189(95), 191(53),179(100)
5, chlorpyrifos-methyl	322	290(2)	212(100)	275(25), 230(85), 227(75), 208(77)
	324	292(2)	214(100)	277(25), 232(95), 229(65), 208(25), 210(40)
	326	294(2)	216(100)	279(25), 234(97), 231(90), 210(45), 212(25)

To further investigate the electronic effects of substituents of the sulfur transfer reaction, compounds **2** and **4** were selected as models for comparison of their CID-MS behaviors. The two potential routes (sulfur transfer versus phenyl ring transfer) to the ions at m/z 154 and m/z 191 in the subsequent fragmentations of corresponding ion **a3** (m/z 232 and m/z 269) were compared by theoretical calculations (Supplementary Material Figures S5 and S6). According to our calculation results, it could be found that the variation trends of key steps on the potential energy surface diagrams for the generation of m/z 154 and m/z 191 are in accordance with those of m/z 169. As shown in Figures S5 and S6, the key steps in route 1 (phenyl migration) and route 2 (sulfur migration) are **TS3** and **TS5**, respectively. For the formation of ions at m/z 154 and m/z 191, the energy barriers of **TS3** and **TS5** follows the order: 193.4 kJ mol^{-1} (**TS3** in route 1) > 155.4 kJ mol^{-1} (**TS5** in route 2) and 214.5 kJ mol^{-1} (**TS3** in route 1) > 166.0 kJ mol^{-1} (**TS5** in route 2), respectively, indicating that sulfur migration is a dynamically more favored process in formation of ions at m/z 154 and m/z 191. These experimental and calculation results of fenthion derivatives indicate the universality and the facility of the sulfur transfer reaction in the dissociation process.

Interestingly, for compounds **2** and **3** with a nitro group on the benzene ring, the intensities of the corresponding **a8** product declined significantly in the CID-MS, indicating the presence of a nitro group, will inhibit the process of sulfur transfer. Thus, the presence of an NO_2 substituent on the phenyl ring inhibits the sulfur transfer reaction, whereas an $-SCH_3$ substituent on the phenyl ring promotes this reaction pathway.

Conclusion

In summary, protonated fenthion derivatives firstly dissociates via the elimination of CH_3OH to generate the predominant fragment ion **a2** (R-phenoxyl, O-methyl phosphonium thioate) upon collisional activation. Then, **a2** further dissociates via the loss of $CH_3O–P=O$ to form the arenesulfenylium cations, R-PhS$^+$. On the basis of the mass spectra data together with isotope labeling experiments and theoretical calculations, an intriguing mechanism via intramolecular stepwise sulfur transfer has been proposed and validated for this fragmentation reaction. Further research is needed to address the gas-phase reactivity of PhS$^+$ and related gas-phase ions.

Acknowledgements

References

1. Vukics, V., Guttman, A.: Structural characterization of flavonoid glycosides by multi-stage mass spectrometry. Mass Spectrom. Rev. **29**, 1–16 (2010)

2. Longevialle, P.: Ion–neutral complexes in the unimolecular reactivity of organic cations in the gas phase. Mass Spectrom. Rev. **11**, 157–192 (1992)

3. Hopfgartner, G., Bourgogne, E.: Quantitative high-throughput analysis of drugs in biological matrices by mass spectrometry. Mass Spectrom. Rev. **22**, 195–214 (2003)

4. Hibbs, J.A., Jariwala, F.B., Weisbecker, C.S., Attygalle, A.B.: Gas-phase fragmentations of anions derived from N-phenyl benzenesulfonamides. J. Am. Soc. Mass Spectrom. **24**, 1280–1287 (2013)

5. Rodriquez, C.F., Cunje, A., Shoeib, T., Chu, I.K., Hopkinson, A.C., Siu, K.W.M.: Proton migration and tautomerism in protonated triglycine. J. Am. Chem. Soc. **123**, 3006–3012 (2001)

6. Herath, K.B., Weisbecker, C.S., Singh, S.B., Attygalle, A.B.: Circumambulatory movement of negative charge ("ring walk") during gas-phase dissociation of 2,3,4-trimethoxybenzoate anion. J. Org. Chem. **79**, 4378–4389 (2014)

7. Zhang, X., Cheng, S.: Intramolecular halogen atom coordinated H transfer *via* ion-neutral complex in the gas phase dissociation of protonated dichlorvos derivatives. J. Am. Soc. Mass Spectrom. **28**, 2246–2254 (2017)

8. Zhang, X., Bai, X., Fang, L., Jiang, K., Li, Z.: Decarboxylative coupling reaction in ESI(−)-MS/MS of 4-nitrobenzyl 4-hydroxybenzoates: triplet ion–neutral complex-mediated 4-nitrobenzyl transfer. J. Am. Soc. Mass Spectrom. **27**, 940–943 (2016)

9. Chai, Y., Xiong, X., Yue, L., Jiang, Y., Pan, Y., Fang, X.: Intramolecular halogen transfer *via* halonium ion intermediates in the gas phase. J. Am. Soc. Mass Spectrom. **27**, 1–7 (2016)

10. Wang, H.Y., Gao, Y., Zhang, F., Yu, C.T., Xu, C., Guo, Y.L.: Mass spectrometric study of the gas-phase difluorocarbene expulsion of polyfluorophenyl cations *via* F-atom migration. J. Am. Soc. Mass Spectrom. **24**, 1919–1926 (2013)

11. Li, F., Zhang, X., Zhang, H., Jiang, K.: Gas-phase fragmentation of the protonated benzyl ester of proline: intramolecular electrophilic substitution *versus* hydride transfer. J. Mass Spectrom. **48**, 423–429 (2013)

12. Wang, H.-Y., Xu, C., Zhu, W., Liu, G.-S., Guo, Y.-L.: Gas phase decarbonylation and cyclization reactions of protonated N-methyl-N-phenylmethacrylamide and its derivatives *via* an amide Claisen rearrangement. J. Am. Soc. Mass Spectrom. **23**, 2149–2157 (2012)

13. George, M., Sebastian, V.S., Reddy, P.N., Srinivas, R., Giblin, D., Gross, M.L.: Gas-phase Nazarov cyclization of protonated 2-methoxy and 2-hydroxychalcone: an example of intramolecular proton-transport catalysis. J. Am. Soc. Mass Spectrom. **20**, 805–818 (2009)

14. Zheng, X., Tao, W.A., Cooks, R.G.: Eberlin reaction of arenesulfenylium cations with cyclic acetals and ketals: ring contraction and cycloreversion. J. Chem. Soc. Perkin Trans. **2**, 350–355 (2001)

15. Wang, S., Dong, C., Yu, L., Guo, C., Jiang, K.: Dissociation of protonated N-(3-phenyl-2H-chromen-2-ylidene)- benzenesulfonamide in the gas phase: cyclization via sulfonyl cation transfer. Rapid Commun. Mass Spectrom. **30**, 95–100 (2016)

16. Wang, S., Yu, L., Wu, Y., Guo, C., Zhang, N., Jiang, K.: Gas-phase fragmentation of protonated N,2-diphenyl-N'-(p-toluenesulfonyl) ethanimidamides: Tosyl cation transfer *versus* proton transfer. J. Am. Soc. Mass Spectrom. **26**, 1428–1431 (2015)

17. Sun, H., Chai, Y., Pan, Y.: Dissociative benzyl cation transfer *versus* proton transfer: loss of benzene from protonated N-benzylaniline. J. Org. Chem. **77**, 7098–8102 (2012)

18. Remeš, M., Roithová, J., Schröder, D., Cope, E.D., Perera, C., Senadheera, S.N., Stensrud, K., Ma, C.-C., Givens, R.S.: Gas-phase fragmentation of deprotonated p-hydroxyphenacyl derivatives. J. Org. Chem. **76**, 2180–2186 (2011)

19. Hu, N., Tu, Y.-P., Jiang, K., Pan, Y.: Intramolecular charge transfer in the gas phase: fragmentation of protonated sulfonamides in mass spectrometry. J. Org. Chem. **75**, 4244–4250 (2010)

20. Hu, N., Tu, Y.-P., Liu, Y., Jiang, K., Pan, Y.: Dissociative protonation and proton transfers: fragmentation of α, β-unsaturated aromatic ketones in mass spectrometry. J. Org. Chem. **73**, 3369–3376 (2008)

21. Tu, Y.-P.: Dissociative protonation sites: reactive centers in protonated molecules leading to fragmentation in mass spectrometry. J. Org. Chem. **71**, 5482–5488 (2006)

22. Hunt, D.F., Giordani, A.B., Shabanowitz, J., Rhodes, G.: Retro-Diels-Alder, γ-hydrogen rearrangement, and decarboxylation reactions. Pathways for fragmentation in the collisions activated dissociation mass spectra of ketones and carboxylic acid $(M-1)^-$ ions. J. Org. Chem. **47**, 738–741 (1982)

23. Kim, J.T., Kel'in, A.V., Gevorgyan, V.: 1,2-migration of the thio group in allenyl sulfides: efficient synthesis of 3-thio-substituted furans and pyrroles. Angew. Chem. Int. Ed. **115**, 102–105 (2003)

24. Bur, S.K.: 1,3-sulfur shifts: mechanism and synthetic utility. In: Schaumann, E. (ed.) Sulfur-Mediated Rearrangements I, pp. 125–171. Springer Berlin Heidelberg, Berlin (2007)

25. Sromek, A.W., Gevorgyan, V.: 1,2-Sulfur migrations. In: Schaumann, E. (ed.) Sulfur-Mediated Rearrangements I, pp. 77–124. Springer Berlin Heidelberg, Berlin (2007)

26. Adam, W., Bargon, R.M.: Synthesis of thiiranes by direct sulfur transfer: the challenge of developing effective sulfur donors and metal catalysts. Chem. Rev. **104**, 251–262 (2004)

27. Fang, Z., Liu, J., Liu, Q., Bi, X.: [3+2] cycloaddition of propargylic alcohols and α-oxo ketene dithioacetals: synthesis of functionalized cyclopentadienes and further application in a Diels–Alder reaction. Angew. Chem. Int. Ed. **53**, 7209–7213 (2014)

28. Dudnik, A.S., Sromek, A.W., Rubina, M., Kim, J.T., Kel'in, A.V., Gevorgyan, V.: Metal-catalyzed 1,2-shift of diverse migrating groups in allenyl systems as a new paradigm toward densely functionalized heterocycles. J. Am. Chem. Soc. **130**, 1440–1452 (2008)

29. Peng, L., Zhang, X., Zhang, S., Wang, J.: Au-catalyzed reaction of propargylic sulfides and dithioacetals. J. Org. Chem. **72**, 1192–1197 (2007)

30. Johnston, B.D., Pinto, B.M.: Synthesis of thio-linked disaccharides by 1→2 intramolecular thioglycosyl migration: Oxacarbenium *versus* episulfonium ion intermediates. J. Org. Chem. **65**, 4607–4617 (2000)

31. Yu, B., Yang, Z.: Stereoselective synthesis of 2-S-phenyl-2-deoxy-β-glycosides using phenyl 2,3-*O*-thiocarbonyl-1-thioglycoside donors *via* 1,2-migration and concurrent glycosidation. Org. Lett. **3**, 377–379 (2001)

32. Peng, L., Zhang, X., Ma, M., Wang, J.: Transition-metal-catalyzed rearrangement of allenyl sulfides: a route to furan derivatives. Angew. Chem. Int. Ed. **119**, 1937–1940 (2007)

33. Eckstein, F., Gish, G.: Phosphorothioates in molecular biology. Trends Biochem. Sci. **14**, 97–100 (1989)

34. Frey, P.A., Sammons, R.D.: Bond order and charge localization in nucleoside phosphorothioates. Science. **228**, 541–545 (1985)

35. Barr, J.D., Bell, A.J., Ferrante, F., La Manna, G., Mundy, J.L., Timperley, C.M., Waters, M.J., Watts, P.: Fragmentations and reactions of some isotopically labelled dimethyl methyl phosphono and trimethyl phosphoro thiolates and thionates studied by electrospray ionisation ion trap mass spectrometry. Int. J. Mass Spectrom. **244**, 29–40 (2005)

36. Kuivalainen, T., Kostiainen, R., Björk, H., Uggla, R., Sundberg, M.R.: Fragmentation of protonated *O,O*-dimethyl *O*-aryl phosphorothionates in tandem mass spectral analysis. J. Am. Soc. Mass Spectrom. **6**, 488–497 (1995)

37. Cooks, R.G., Gerrard, A.F.: Electron impact-induced rearrangements in compounds having the P=S bond. J. Chem. Soc. B. 1327–1333 (1968)

38. Santoro, E.: The fragmentation of some alkyl thio-phosphate esters by electron-impact. Org. Mass Spectrom. **7**, 589–599 (1973)

39. Zeller, L.C., Farrell, J.T., Kenttämaa, H.I., Kuivalainen, T.: Multiple-stage mass spectrometry in structural characterization of organophosphorus compounds. J. Am. Soc. Mass Spectrom. **4**, 125–134 (1993)

40. Deng, M., Yu, T., Luo, H., Zhu, T., Huang, X., Luo, L.: Direct detection of multiple pesticides in honey by neutral desorption-extractive electrospray ionization mass spectrometry. Int. J. Mass Spectrom. **422**, 111–118 (2017)

41. Picó, Y., Farré, M., Soler, C., Barceló, D.: Confirmation of fenthion metabolites in oranges by IT-MS and QqTOF-MS. Anal. Chem. **79**, 9350–9363 (2007)

42. Frisch, M., Trucks, G.W., Schlegel, H.B., Scuseria, G.E., Robb, M.A., Cheeseman, J.R., Zakrzewski, V.G., Montgomery Jr., J.A., Stratmann, R.E., Burant, J.C., Dapprich, S., Millam, J.M., Daniels, A.D., Kudin, K.N., Strain, M.C., Farkas, O., Tomasi, J., Barone, V., Cossi, M., Cammi, R., Mennucci, B., Pomelli, C., Adamo, C., Clifford, S., Ochterski, J., Petersson, G.A., Ayala, P.Y., Cui, Q., Morokuma, K., Malick, D.K., Rabuck, A.D., Raghavachari, K., Foresman, J.B., Cioslowski, J., Ortiz, J.V., Stefanov, B.B., Liu, G., Liashenko, A., Piskorz, P., Komaromi, I., Gomperts, R., Martin, R.L., Fox, D.J., Keith, T., Al-Laham, M.A., Peng, C.Y., Nanayakkara, A., Gonzalez, C., Challacombe, M., Gill, P.M.W., Johnson, B., Chen, W., Wong, M.W., Andres, J.L., Gonzalez, C., Head-Gordon, M.E., Replogle, S., Pople, J.A.: Gaussian 03, Revision B.03. Gaussian, Inc., Wallingford (2004)

43. Bortolini, O., Guerrini, A., Lucchini, V., Modena, G., Pasquato, L.: The phenylsulfenium cation: electronic structure and gas-phase reactivity. Tetrahedron Lett. **40**, 6073–6076 (1999)

44. Smit, W.A., Krimer, M.Z., Vorob'eva, E.A.: Generation and chemical reactions of episolfonium ions. Tetrahedron Lett. **16**, 2451–2454 (1975)

45. Matsumoto, K., Kozuki, Y., Ashikari, Y., Suga, S., Kashimura, S., Yoshida, J.-I.: Electrophilic substitution reactions using an electrogenerated $ArS(ArSSAr)^+$ cation pool as an ArS^+ equivalent. Tetrahedron Lett. **53**, 1916–1919 (2012)

46. Verhaeghe, P., Dumètre, A., Castera-Ducros, C., Hutter, S., Laget, M., Fersing, C., Prieri, M., Yzombard, J., Sifredi, F., Rault, S., Rathelot, P., Vanelle, P., Azas, N.: 4-Thiophenoxy-2-trichloromethyquinazolines display in vitro selective antiplasmodial activity against the human malaria parasite *Plasmodium falciparum*. Bioorg. Med. Chem. Lett. **21**, 6003–6006 (2011)

47. Niddam, V., Camplo, M., Le Nguyen, D., Chermann, J.-C., Kraus, J.-L.: Thiophenoxy peptides: a new class of HIV replication inhibitors. Bioorg. Med. Chem. Lett. **6**, 609–614 (1996)

48. Medou, M., Priem, G., Rocheblave, L., Pepe, G., Meyer, M., Chermann, J.-C., Kraus, J.-L.: Synthesis and anti-HIV activity of α-thiophenoxy-hydroxyethylamide derivatives. Eur. J. Med. Chem. **34**, 625–638 (1999)

49. Jiang, K., Bian, G., Hu, N., Pan, Y., Lai, G.: Coordinated dissociative proton transfers of external proton and thiocarbamide hydrogen: MS experimental and theoretical studies on the fragmentation of protonated *S*-methyl benzenylmethylenehydrazine dithiocarboxylate in gas phase. Int. J. Mass Spectrom. **291**, 17–23 (2010)

50. Kuck, D., Bather, W.: Inter- and intra-annular proton exchange in gaseous benzylbenzenium ions (protonated diphenylmethane). Org. Mass Spectrom. **21**, 451–457 (1986)

51. Newman, M.S., Karnes, H.A.: The conversion of phenols to thiophenols *via* dialkylthiocarbamates. J. Org. Chem. **31**, 3980–3984 (1966)

52. Prabhakar, S., Kar, P., Mirza, S.P., Lakshmi, V.V.S., Nagaiah, K., Vairamani, M.: Mass spectral study of *O*- and *S*-aryl dimethylthiocarbamates under electron impact conditions: Newman-Kwart rearrangement in the gas phase. Rapid Commun. Mass Spectrom. **15**, 2127–2134 (2001)